Physicochem. Probl. Miner. Process., 56(7), 2021, 95-101

http://www.journalssystem.com/ppmp

Physicochemical Problems of Mineral Processing

ISSN 1643-1049

Received June 02, 2021; reviewed; accepted October 07, 2021

Exploitation of spent nickel-metal hydride (Ni-MH) batteries as a source of value-added products

Fatma E. Farghal, Mohamed A. Abdel-Khalek

Central Metallurgical Research and Development Institute (CMRDI), P.O. Box 87, Helwan 11421, Cairo, Egypt

Corresponding author: femam66@yahoo.com (F. E. Farghal)

Abstract: Spent Nickel–metal hydride batteries can be sources of valuable metals such as nickel, cobalt, manganese, rare earths and toxic chemicals. The recycling of these materials is necessary from both economic and environmental points of view. In this study the nickel is leached in acid solution followed by precipitation and thermal decomposition or by cementation. The affecting parameters such as acid type and concentration, time, temperature and solid/liquid ratio were investigated. The maximum of leached nickel could be obtained in 3M sulfuric acid at 65°C for 60 min with solid-to-liquid ratio of 30 g L^{-1}. The liquid film is a more suitable model for demonstrating the kinetics of the nickel leaching. Thermal decomposition of the precipitated nickel dimethyl-glyoxime was employed in preparation of nickel oxide. Nickel was separated from aqueous solution by cementation on zinc. The cementation process follows pseudo first-order kinetics and diffusion controlling steps. The yield was 91% of the original nickel content.

Keywords: nickel–metal hydride, batteries, nickel, recovery, cementation, leaching, recycling

1. Introduction

Electrical and electronic equipment production is fast growing due to their increased use and the high-cost of repair. Thus, large amounts of obsolete equipment generate a lot of electronic waste (Strada-Ruiz et al., 2016; Porvali et al., 2019). The electronic equipment and mobile phones have a short lifespan of less than 3 years (Kasper et al., 2011; Jing-Ying et al., 2012). It needs recycling not only for environmental concerns, but also for economic reasons. The electronic wastes contain significant amounts of valuable metals such as copper, lead, tin, zinc, etc. The recycling has two goals, first, the reduction of e-waste generated and pollution associated with them and second, the recovery of valuable metals (Veit et al., 2006; Kim et al., 2011; Cayumil et al., 2014). Separation of different materials of printed circuit boards by physical processes such as sizing, density separation, magnetic separation, liquid-solid fluidization, flotation and bioflotation can be employed in sustainable separation processes (Abdel-Khalek and El-Midany, 2013; Zhao et al., 2017; Mesbah et al., 2020; Rinne et al., 2021).

The mobile phone contains about 63% metal, 24% ceramic, and 13% polymer, depending on the age and model of the phone (Yamane et al., 2011). The construction of Ni-MH cell is similar to that of corresponding nickel-cadmium cells. In Ni-MH battery, cadmium electrode is replaced by a hydrogen storage alloy, where it is employed for the cathode, along with nickel hydroxide for the anode, and alkali-resistant nylon non-woven fabric as in Ni-Cd batteries, poly-propylene non-woven fabric and polyamide non-woven fabric for the separator. The Ni-MH batteries contain valuable metals (44% nickel, 5% cobalt, 2% zinc and about 9% light rare earth metals (Shin et al., 2015). The highest contents were found for Ni, Fe, and La, followed by Ce, Co, K, Na, Zn, and Mn. The nickel was found in the cathode metal, while the cobalt was mainly in the anode metal. A preliminary economic analysis evaluated the recovery of valuable metals from spent NiMH batteries using thermal melting versus simple mechanical separation. The estimated profits of recovering valuable metals from NiMH batteries by using thermal melting and mechanical processing are 2,329 and 2,531 USD/ton, respectively. (Lin et

DOI: 10.37190/ppmp/142929

al., 2015). Acid leaching is time consuming while by employing supercritical CO_2, with H_2O_2 and H_2SO_4 as co-solvents, the leaching rate is higher. The supercritical extraction provided more selective recovery such as copper compared to tin from printed circuit (Calgaro et al., 2015).

Citric acid and hydrogen peroxide were used for extraction of the valuable metals from spent lithium-ion batteries at 80°C (Chen and Zhou, 2014). Rare earths, nickel, and cobalt were recovered from hybrid electric vehicle batteries by sulfation, roasting, and water leaching in 8 M sulfuric acid with solid-liquid ratio of 1/5. Rare earth elements could be extracted without nickel and cobalt contamination after roasting at 850°C for 2 h. The Ni and Co remain in the solid phase as oxides together with aluminum, zinc, and iron (Korkmaz et al., 2018).

Diphonix resin could adsorb nickel and lanthanum ions from the leached nickel-metal hydride batteries (Ni-MH) in 0.2 M HNO_3 acid solution (Fila et al.,2019). The rare earth metals could be separated by solvent extraction in bis(2-ethylhexyl) phosphoric then cobalt and nickel are recovered as oxalates (Pradhan et al., 2021). Simultaneous electrolysis could be used, together with the precipitated rare earths for fresh hydrogen-storage alloys production (Kleinsorgen et al., 1999).

This work aims to investigate the recycling of nickel from spent of the Panasonic Prismatic Module nickel metal hydride (Ni-MH) battery to produce a value-added product as nickel metal and nickel oxide.

2. Materials and methods

2.1. Materials

Spent nickel-metal hydride (Ni-MH) batteries were collected from local market. All chemicals used such as sulfuric, nitric and hydrochloric acids, Dimethyl glyoxime, and zinc powder were supplied by Merck of analytical grade.

2.2. Methods

2.2.1. Waste battery preparation

Ni-MH batteries were cut in half longitudinally to separate the metal cover from the internal components include the electrodes and nylon between the electrodes. The crushed product was ground to less than 1 mm particle size. The valuable fine powder was separated by sieving, which has a particle size less than 0.1 mm. The steel pieces and plastics remained in the oversize while the fine contains the valuable metals. The fine fraction was washed to remove alkaline electrolyte present in these batteries (Porvali et al., 2020).

2.2.2. Leaching studies

Leaching was carried out by adding 30g of the battery scrap powder in 50 ml of HCl, HNO_3 or H_2SO_4 solutions of different concentration (0.5 – 4 M) in a 100-ml beaker. The mixing was carried out using a magnetic bar. After 60 min the leached solution was separated through filtration.

2.2.3. Precipitation and thermal decomposition

Nickel was separated by precipitation as nickel dimethyl-glyoxime. It was carried out by adding 1% dimethylglyoxime to leached solution at pH 5 then heat to 80°C for 15 min. After cooling, filter the solution and test the filtrate for the completeness of precipitation. Dry the precipitate in an oven at 130°C for one hour. Thermal decomposition of nickel dimethyl-glyoxime was carried out in muffle at 400°C for one hour to produce nickel oxide. Also, another 10g of nickel dimethyl-glyoxime was re- dissolved in 20ml of concentrated hydrochloric acid solution and then diluted with water up to 100ml for cementation process.

2.2.4. Cementation process

A zinc powder was used to cement Ni^{2+} ions from aqueous solution which produced as a result of dissolving the nickel bis(dimethyl-glyoximate) in acid solution. The cementation was carried out in a cylindrical glass reactor with a cylindrical stainless-steel agitator which is connected to a variable speed

motor. They are isolated with epoxy resin. The temperature was controlled using a water bath. Zinc powder is used for nickel cementation at pH 2.5. After interval times a 2 ml of the solution is taken, filtered and chemically analyzed.

2.2.5. Characterization

The complete chemical analysis of the battery scrap powder was carried out using X-ray fluorescence "Rigakusuper Mini 200" X-ray fluorescence. The sample was pressed into a pellet through mixing the sample with Boreox BM-0008 binder and the mixture were subjected to 20 tons press using "Fluxana PR-25N" for 20 Sec. Atomic absorption, Perkin Elmer AAnalyst 200 was employed for determination of nickel in leached solution. For nickel oxide, it is determined after dissolution in KCN. The surface morphology and microstructure of products were identified by JEOL instrument (Japan) model JSM-5410 scanning electron microscope (SEM) at 15 kV of excitation potential.

3. Results and discussion

3.1. Chemical composition of Ni-MH batteries

Table 1 shows the battery components and their availability. Table 2 shows the chemical composition of Ni battery components. According to the chemical analysis result, it contains about 44% nickel (Ni), 9% lanthanum (La) and 3% cerium (Ce).

Table 1. Chemical composition of (Ni-MH) battery

Component	Wt.%
Metalliccases	55.1
Battery paste	37.5
Membrane and plastics	4.26
Electrolyte	2.82
Remainder	0.32

Table 2. Metal ions concentration in Ni-battery

Metal	Ni	La	K	Co	Mn	Ce	Zn	Al	Fe	Cd	Li
%	44.23	9.12	8.64	4.96	2.98	2.78	2.47	0.874	0.34	0.17	0.13

3.2. Leaching of nickel

The most affecting parameters of the leaching process such as acid type and concentration and quantity of cell powder, time and temperature were investigated.

3.2.1. Effect of acid type and concentration

Fig. 1 shows the effect of acid concentration and type on nickel extraction efficiency. The extraction increases with increasing acid concentration of all acids. About 90% of nickel could be extracted in 3 - 4M sulfuric acid at 25°C for 60 min. The extraction efficiency of hydrochloric and nitric acids was 70% and 35%, respectively. Sulfation and leaching are shown to be a viable option for separation of the rare earths from cobalt and nickel present in the Ni-MH batteries. At a higher acid concentration, the recovery of rare earths decreases due to the formation of oxy-sulfates that will remain in the solid phase. The optimal sulfuric acid concentration in the sulfation step was determined to be 3 M for a solid-to-liquid ratio of 30 g L^{-1} (Korkmaz et al., 2018).

3.2.2. Effect of cell powder auantity

Fig. 2 shows the effect of quantity of cell powder on the dissolution of Ni at different concentration of sulfuric acid at 60 min. The dissolution is increased with increasing the acid concentration. In contrast,

the dissolution of Ni is decreased with increasing the quantity of cell powder at 0.5 M acid. This is may be due to insufficient acid species to attack nickel atoms at this lower acid concentration.

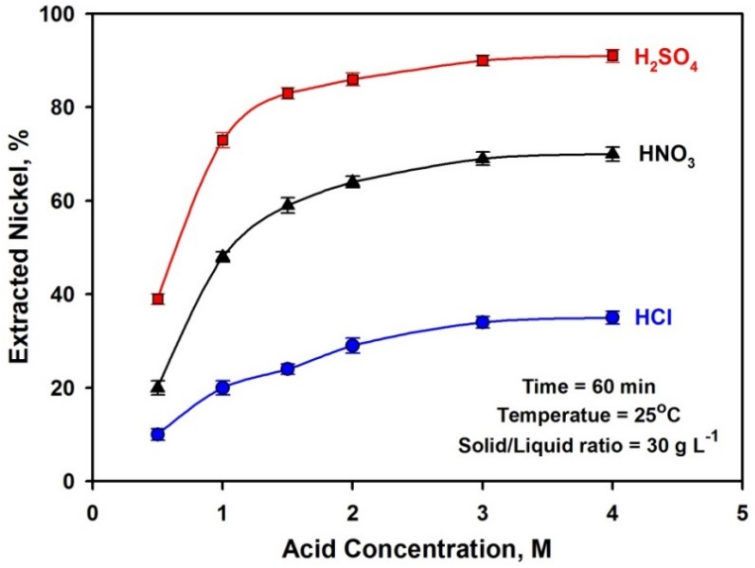

Fig. 1. Effect of acid type and concentration on leaching process

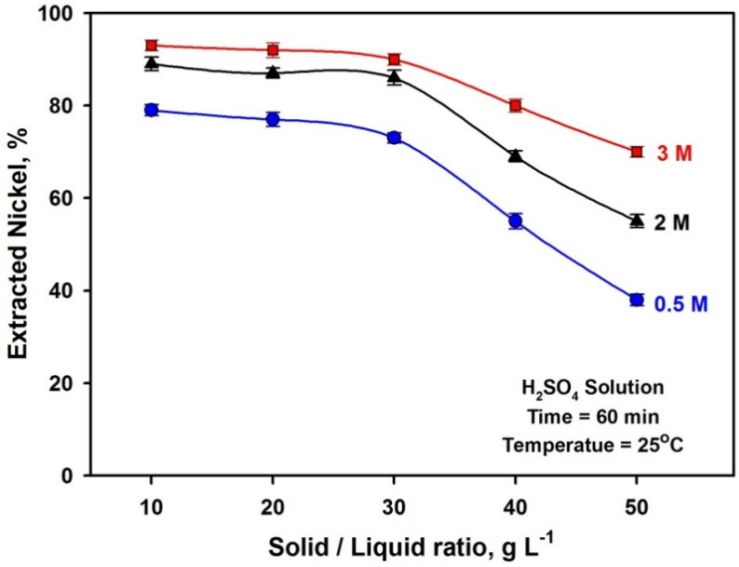

Fig. 2. Effect of solid/liquid ratio on nickel dissolution as a function of H_2SO_4 concentration

3.2.3. Effect of leaching time and temperature

Fig. 3 shows the effect of contact time on Ni dissolution as a function of acid concentration. The Ni dissolution increases with increasing time. The maximum dissolution of nickel is achieved after 60 min. The higher initial rate up to 30 min. It is due to continuous oxidation of metal atoms to metal ions. The decreasing rate after 50 min may be due decreasing oxidation rate. Different metals present in the raw material reduced the hydrogen in acidic solution, with a vigorous gas generation during leaching (Porvali et al., 2020). Fig. 4 shows the effect of leaching time on nickel extraction as a function of temperature. The nickel dissolution slightly increases with increasing temperature. It may be due to the exothermic nature of the leaching process (Tzanetakis and Scott, 2004). These results suggest that the waste has highly reductive properties due to gas evolution. The limited acidity leads a selective dissolution. Iron and aluminum were observed to begin to dissolve only after significant dissolution of rare earths, nickel and cobalt. The rare earths were precipitated as double salts, so the rare earths were not expected to be in the leached solution (Porvali et al., 2020).

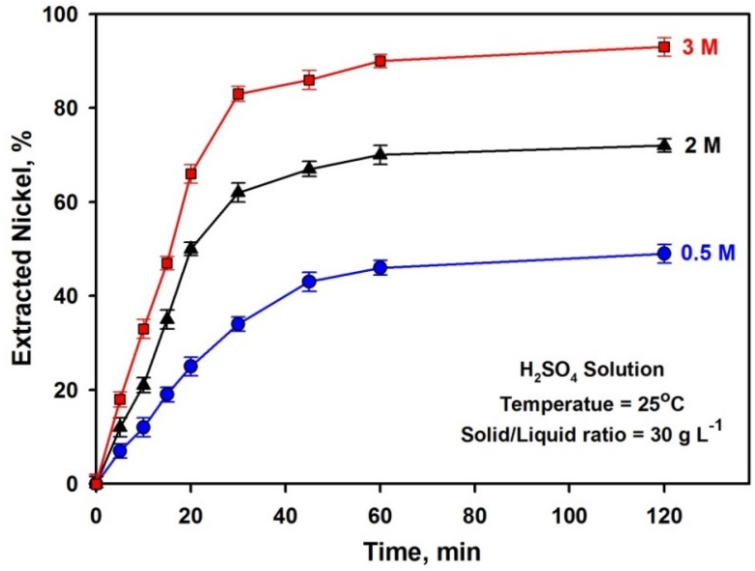

Fig. 3. Effect of leaching time on nickel extraction as a function of H_2SO_4 concentration

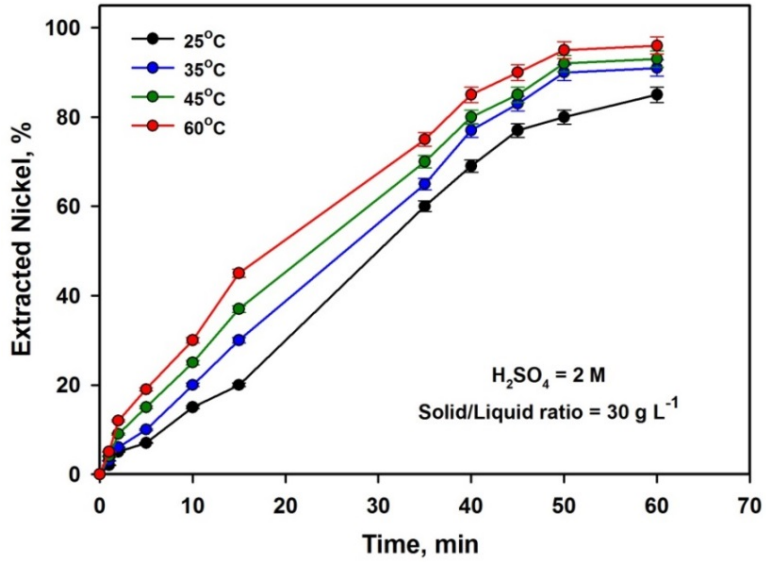

Fig. 4. Effect of leaching time on nickel extraction as a function of temperature

3.2.4. Kinetic Study

The leaching of nickel in acid is expressed as:

$$aA_{liquid} + bB_{solid} = \text{Product} \quad (1)$$

where a, b, A and B represent the stoichiometric coefficients. The kinetics of the reaction are described by using the shrinking core model. According this model the solid is initially surrounded by a fluid film through which the mass is transferred between the solid and the bulk solution. As the reaction proceeds, the unreacted solid shrinks towards the solid center, and a layer of porous product forms around the unreacted solid. If the reaction is controlled by diffusion through a liquid film, the integrated rate equation is:

$$X = K_1 t \quad (2)$$

If the reaction is controlled by a surface chemical reaction, the integrated rate equation is:

$$1 - (1 - X)^{1/3} = K_r t \quad (3)$$

If the reaction is controlled by diffusion through a product layer, the integrated rate equation is:

$$1 - 3\,(1 - X)^{2/3} + 2\,(1 - X) = K_d t \quad (4)$$

If the reaction is controlled by mixed kinetic model, the integrated rate equation is:

$$[1 - (1 - X)^{1/3}]^2 = K_m t \quad (5)$$

where X is the conversion fraction of solid particles, K_l is the apparent rate constant for the liquid film, K_r is the apparent rate constant of the surface chemical reaction, K_d is the apparent rate constant for the diffusion through a product layer, K_m is the apparent rate constant for the mixed kinetic model and t is the reaction time.

To determine the kinetic parameters and rate controlling step of nickel leaching, the experimental data were analyzed using the above models. Figs. 5, 6, 7 and 8 showed that based on the values of R^2, show that the liquid film model best described the acid leaching process than that of other models. In the earlier stages of the leaching process, the acid ions migrate from the solution to the external surface of the metal. Then, it was followed by the diffusion through the boundary layer of the active sites. Finally, the intraparticle diffusion and adsorption in the inner part of the metal occurred. According to the liquid-film diffusion model, the flow of the acid ions through a liquid film surrounding the metal surface is the rate-determining step. While at high temperature, the Ni leaching was increased, but the leaching rate was not linear with time, indicating that boundary layer diffusion was not the main control step in the acid leaching process and surface chemical reaction may predominates.

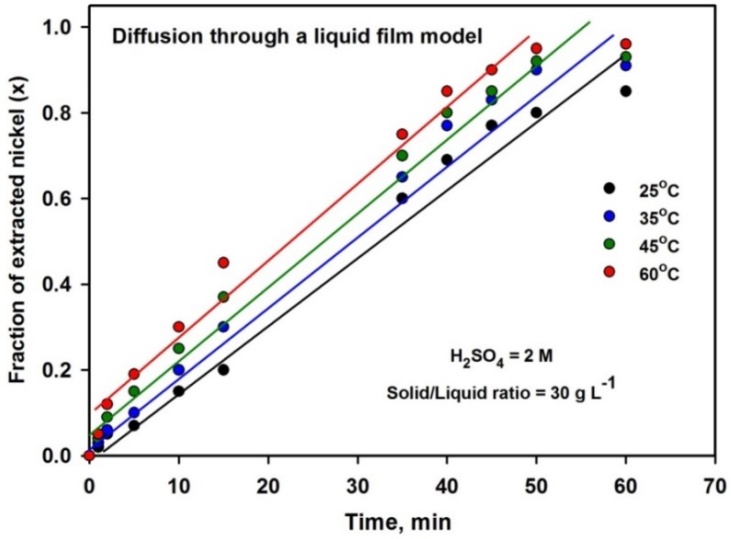

Fig. 5. Fitting the results by the diffusion through a liquid film model

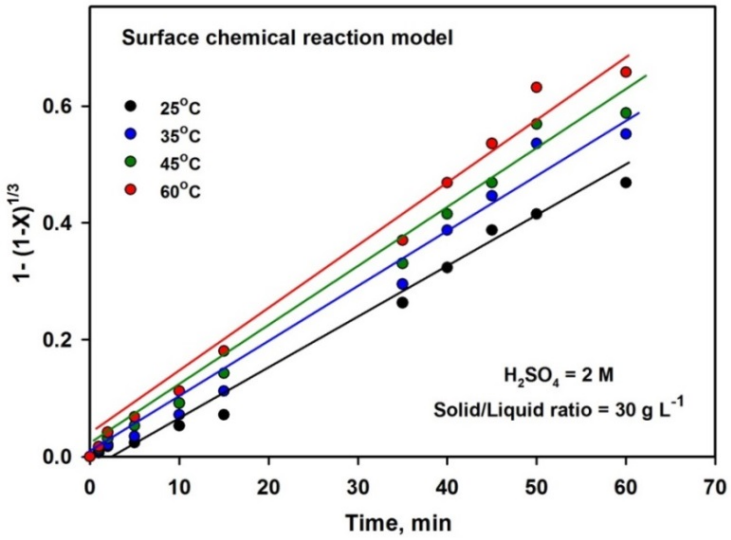

Fig. 6. Fitting the results by the surface chemical reaction model

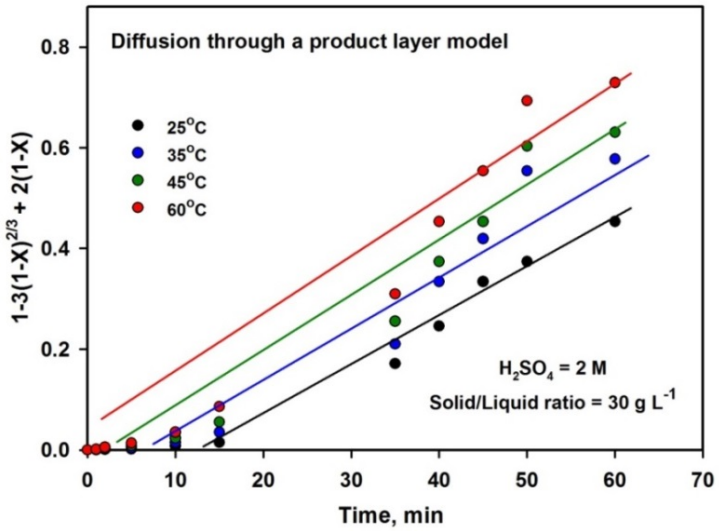

Fig. 7. Fitting the results by the diffusion through a product layer model

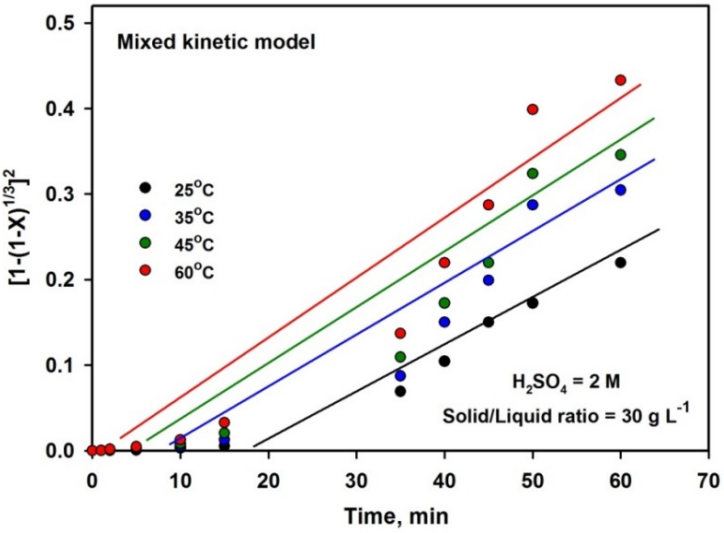

Fig. 8. Fitting the results by the diffusion through a liquid film model

Table 3. The kinetic parameters and rate controlling step of nickel leaching

Model	Parameter	25°C	35°C	45°C	60°C
Diffusion through a liquid film	R^2	**0.9965**	**0.9930**	**0.9873**	**0.9853**
	K_1	0.0157	0.0162	0.0165	0.0169
Surface chemical reaction	R^2	0.9513	0.9423	0.9404	0.9326
	K_r	0.0083	0.0099	0.0103	0.0114
Diffusion through a product layer	R^2	0.9465	0.9369	0.9342	0.9206
	K_d	0.0077	0.0102	0.0111	0.0129
Mixed kinetic model	R^2	0.8316	0.8297	0.8216	0.8133
	K_m	0.0036	0.0052	0.0058	0.0073

3.3. Thermal decomposition

Fig. 9 shows the thermal decomposition of the nickel dimethylglyoxime precipitate up to 400°C for 1 hr. The weight loss increases with increasing temperature. A weight loss of about 74-74.2% is achieved at

350-400°C. Uniform single-crystalline NiO particles are successfully obtained. The typical SEM image (Fig. 10) shows that the building block possesses a well-defined uniform octahedral structure with a highly symmetric, regular shape, which exhibits sharp edges and corners as well as smooth surfaces (Yao et al., 2020).

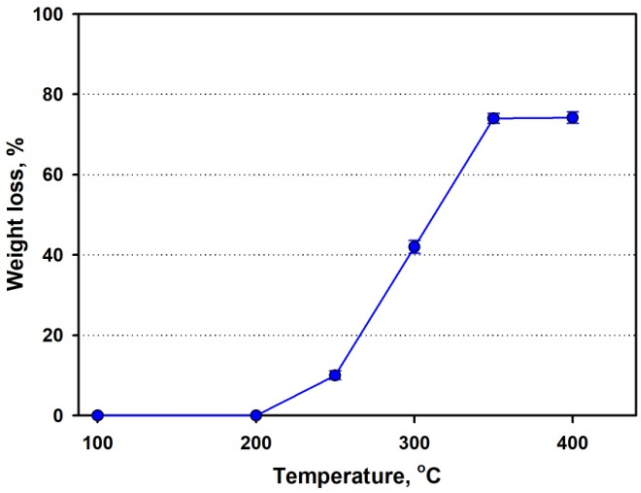

Fig. 9. Thermal decomposition of nickel dimethylglyoxime to nickel oxide

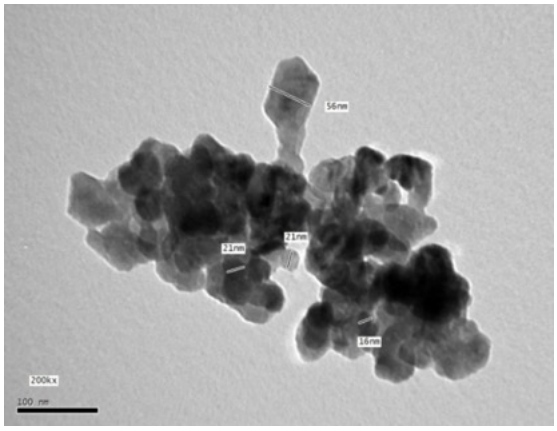

Fig. 10. SEM images of the obtained nickel oxide

3.4. Cementation of Nickel

The nickel ions were separated from the nickel solution by cementation on zinc through its reduction to metallic form. Fig. 11 shows the effect of the stoichiometric amount of added zinc metal and time on the nickel recovery. The nickel recovery increases with increasing both the amount of added zinc and time. The initial rate of cementation is higher at a higher stoichiometric ratio of zinc metal. Increasing of zinc particles overcomes the resistance to mass transfer of nickel ions between the aqueous phase and the solid surface of zinc metal particles (Bhattacharyya and Gupta, 2006).

To explain the mechanism of this reaction, the kinetic models such as pseudo-first & second-order kinetic models were employed. To plot the experimental data, the following integral forms of the models were applied. It means that the plotting of each form should give a straight line in the right order (El-Hosiny et al., 2018).

$$\text{Pseudo-first-order model} \quad \mathbf{\ln[C_e] = \ln [C_o] - K_1 t} \tag{6}$$

$$\text{Pseudo-second-order model} \quad \mathbf{1/[C_e] = 1/[C_o] + K_2 t} \tag{7}$$

where, C_e is the equilibrium nickel ion concentration at time t (the residual concentration of nickel ions) and C_o is the initial concentration of nickel ions. The rate constants for pseudo-first-order and pseudo-second-order models are "K_1"and "K_2".

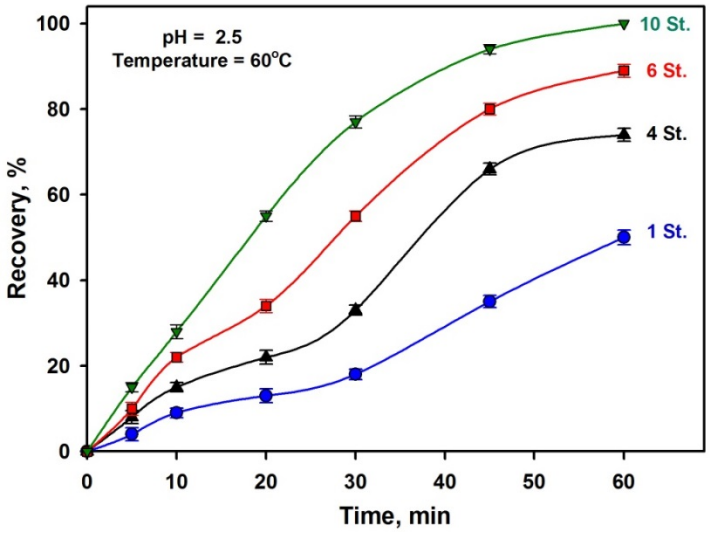

Fig. 11. Effect of cementation time on the recovery of nickel metal as a function of zinc addition

Fig. 12a shows the plot of ln[C_e] versus *t* which gives a straight line for pseudo-first-order adsorption kinetics. It allows computation of the rate constant K_1 with high linear regression coefficient (R^2) ≥ 0.98. It suggests that the process follows pseudo first-order kinetics, Table 4. The plotting of 1/[C_e] versus time t (Fig. 12b) gives a straight line with low linear regression coefficient (R^2) = 0.76 – 0.79. It allows computation of the rate constant K_2. It suggests that the process doesn't follow pseudo second-order kinetics. These results agree the reported results which stated that the cementation reaction followed first-order kinetics and diffusion controlling steps (Abdel-Rahman and Abdel-Wahed, 2012).

SEM micrograph of the produced nickel is shown in Fig. 13. The deposit morphology of nickel was found to be dendritic. The dendrites create a local surface roughness which induce the formation of eddies. These eddies enhance the rate of nickel cementation (Abdel-Rahman and Abdel-Wahed, 2012).

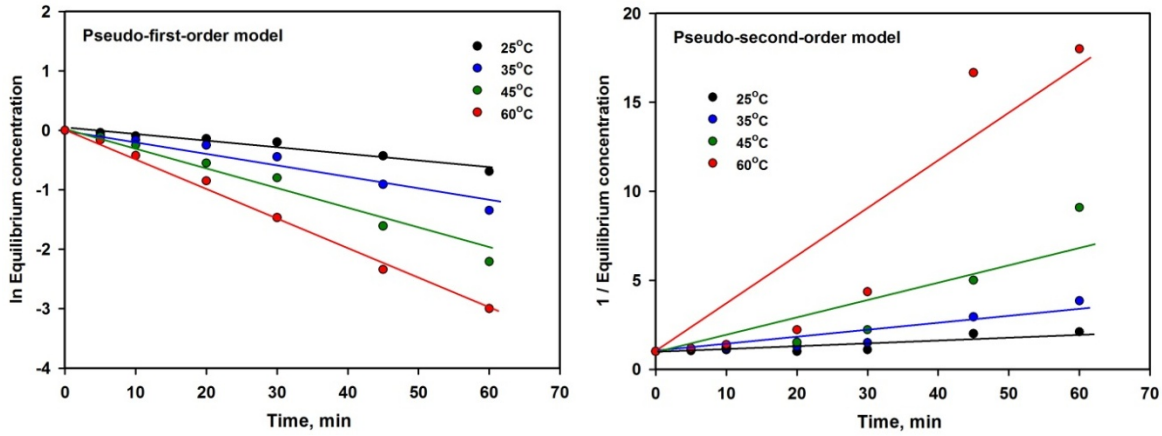

Fig. 12. Plotting of pseudo-first and second order kinetic models

Table 4. Pseudo-first and second order kinetic constants.

Model	Parameter	Stoichiometric amount of zinc			
		1 St..	4 St.	6 St.	10 St.
First order	**R^2**	**0.9893**	**0.9836**	**0.9783**	**0.9756**
	K_1	-0.0109	-0.0231	-0.0374	-0.0618
Second order	**R^2**	0.7962	0.7843	0.7754	0.7698
	K_2	0.0154	0.0476	0.0126	0.0316

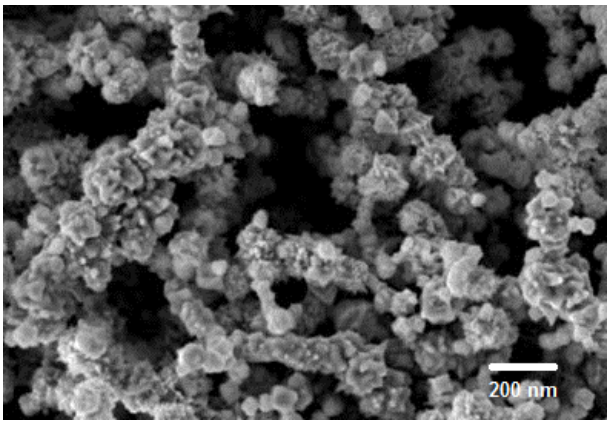

Fig. 13. SEM image of the obtained nickel metal

4. Conclusions

The Ni-MH batteries contain about 44% nickel. It has highly reductive properties with gas evolution. The extraction efficiency of nickel in nitric and hydrochloric acids was 35% and 70%, respectively. The maximum leached nickel of about 93% could be obtained in 3 M sulfuric acid at 65°C for 60 min with solid-to-liquid ratio of 30 g L^{-1}. The leaching slightly increases with increasing temperature.

The kinetics of leaching process are described by the shrinking core model. The liquid film is a more suitable model for demonstrating the kinetics of the nickel leaching system. The maximum thermal decomposition of the precipitated nickel dimethylglyoxime precipitate was achieved at about 350 - 400°C for 1 hr.

Nickel oxide particles were successfully obtained with uniform octahedral structure. Also, the nickel metal was separated from the nickel solution by cementation on zinc. The nickel recovery depended on the amount of the zinc amount and cementation time. The initial rate of cementation is higher at a higher stoichiometric ratio of zinc metal. The cementation process followed first-order kinetics and diffusion controlling steps. The morphology of the prepared nickel to be dendritic. The recovery of the whole processes was about 91%.

References

ABDEL-RAHMAN H.H., ABDEL-WAHED E.M., 2012. *Removal of nickel ions by cementation on zinc from $NiSO_4$ solution in presence of accelerator non-toxic organic compounds*. Hydrometallurgy, 129–130, 111-117.

ABDEL-KHALEK M.A., EL-MIDANY A.A., 2013. *Application of Bacillus subtilis for reducing ash and sulfur in coal*. Environ Earth Sci. 70, 753–760 (2013).

AGARWAL V., KHALID M.K., PORVALI A., WILSON B.P., LUNDSTROM M., 2019. *Recycling of spent Ni-MH batteries: Integration of battery leach solution into primary Ni production using solvent extraction*. Sustainable Materials and Technologies, 22, 121.

BHATTACHARYYA K.G., GUPTA S.S., 2006. *Adsorption of Fe(III) from water by natural & acid activated clays: Studies on equilibrium isotherm, kinetics and thermodynamics of interactions*. Adsorption, 12, 185–204.

CALGARO C.O., SCHLEMMER D.F., DA SILVA M.D.C.R., MAZIERO E.V., TANABE E.H., BERTUOL D.A., 2015. *Fast copper extraction from printed circuit boards using supercritical carbon dioxide*. Waste Manag., 45,289-297.

CAYUMIL R., KHANNA R., IKRAM-Ul-HAQ M., RAJARAO R., HILL A., SAHAJWALLA V., 2014. *Generation of copper rich metallic phases from waste printed circuit boards,* Waste Manage., 34, 1783-1792.

CHEN X., ZHOU T., 2014. *Hydrometallurgical process for the recovery of metal values from spent lithium-ion batteries in citric acid media*. Waste Manag. Res., 32, 11, 1083-1093.

EL-HOSINY F.I., SELIM K.A, ABDEL-KHALEK M.A., OSAMA I., 2018. *Physicochemical study of dye removal using electro-coagulation-flotation process*. Physicochem. Probl. Miner. Process. 2018, 54, 2, 321–333.

FILA D., HUBICIKI Z., KOLODYNSKA D., 2019. *Recovery of metals from waste nickel-metal hydride batteries using multifunctional Diphonix resin*. Adsorption 25, 367–382.

JING-YING L., XIU-LI X., WEN-QUAN L., 2012. *Thiourea leaching gold and silver from the printed circuit boardsof waste mobile phones.* Waste Manage., 32, 1209-1212.

KASPER A.C., BERSELLI G.B.T., FREITAS B.D., TENORIO J.A.S., BERNARDES A.M., VEIT H.M., 2011. *Printed wiring boards for mobile phones: characterization and recycling of copper*. Waste Manage., 31, 2536-2545.

KIM E.Y., KIM M.S., LEE J.C., JEONG J., PANDEY B.D., 2011. *Leaching kinetics of copper from waste printed circuit boards by electrogenerated chlorine in HCl solution.* Hydrometallurgy, 107, 124-132.

KLEINSORGEN K., KOHLER U., BOUVIER A., FOLZER A., 1999. *Process for the recovery of metals from used nickel/metal hydride storage batteries.* Patent US5858061A United States.

KORKMAZ K., ALEMRAJABI M., RASMUSON A., FORSBERG K., 2018. *Recoveries of Valuable Metals from Spent Nickel Metal Hydride Vehicle Batteries via Sulfation, Selective Roasting, and Water Leaching*. Journal of Sustainable Metallurgy, 4, 3, 313-325.

LIN S.L., HUANG K.L., WANG I.C., CHOU I.C., KUO Y.M., HUNG C.H., LIN C., 2015. *Characterization of Spent Nickel-Metal Hydride Batteries and a Preliminary Economic Evaluation of the Recovery Processes.* Journal of the Air & Waste Management Association, 66, 3.

MESBAH Y.I., AHMED N., ALI B.A., ALLAM N.K., 2020. *Recycling of Li-Ni-Mn-Co Hydroxide from Spent Batteries to Produce High-Performance Super capacitors with Exceptional Stability*. Chem. Electro. Chem., 7, 4, 975-982.

PORVALI A., ALTONEN M., OJANEN S., VELAZQUEZ-MARTINEZ O., ERONEN E., LIU F., WILSON B.P., SERNA-GUERREO R., LUNDSTROM M., 2019. *Mechanical and hydrometallurgical processes in HCl media for the recycling of valuable metals from Li-ion battery waste. Resources.* Conservation and Recycling, 142, 257-266.

PORVALI A., OJANEN S., WILSON B.P., SERNA-GUEERRERO R., LUNDSTROM M., 2020. *Nickel metal hydride battery waste: Mechano-hydrometallurgical experimental study on recycling aspects.* J. Sustain. Metall. 6, 78–90.

PRADHAN S., NAYAK R., MISHRA S., 2021. *A review on the recovery of metal values from spent nickel metal hydride and lithium-ion batteries.* Int. J. Environ. Sci. Technol.

RINNE M., ELOMAA H., PORVALI A., LUNDSTROM M., 2021. *Simulation-based life cycle assessment for hydrometallurgical recycling of mixed LIB and Ni-MH waste.* Resources, Conservation and Recycling, 170.

SHIN S.M., SHIN D.J., JUNG G.J., KIM Y.H., WANG J.P., 2015. *Recovery of electronic powder from spent nickel-metal hydride batteries (Ni-MH).* Archives of metallurgy and materials, 60, 2, 1139-1143.

STRADA-RUIZ R.H., FLORES-CAMPOS R., GAMEZ-ALTAMIRANO H.A., VELARDE-SANCHEZ E.J., 2016. *Separation of the metallic and non-metallic fraction from printed circuit boards employing green technology*. J. Hazard. Mater., 311, 91-99.

TZANETAKIS N., SCOTT K., 2004. *Recycling of nickel–metal hydride batteries: dissolution and solvent extraction of metals.* J. of Chemical Technology and Biotechnology, 79, 919–926.

VEIT H.M., BERNARDES A.M., FERREIRA J.Z., TENORIO J.A.S., MALFATTI C.F., 2006. *Recovery of copper from printed circuit boards scraps by mechanical processing and electrometallurgy.* J. Hazard. Mater., B137, 1704-1709.

YAMANE L.H., MORAES V.T., ESPINOSA D.C.R., TENORIO J.A.S., 2011. *Recycling of WEEE: characterization of spent printed circuit boards from mobile phones and computers*. Waste Manage., 31, 2553-2558.

YAO E., XU S., ZHAO F., HUANG T., LI H., ZHAO N., YI J., YANG Y., WANG C. 2020. *Study on thermal decomposition behavior, gaseous products & kinetic analysis of bis-(dimethylglyoxime) nickel complex using TG-DSC-FTIR-MS technique.* Catalysts, 10, 331.

ZHAO C., ZHANG X., DING J., ZHU Y., 2017. *Study on recovery of valuable metals from waste mobile phone PCB particles using liquid-solid fluidization technique*. Chem. Eng. J., 311, 217-226.